Journal of California and Great Basin Anthropology | Vol. 34, No. 2 (2014) | pp. 273–286

REPORTS

Obsidian Re-Use at the Rose Spring Site (CA-INY-372), Eastern California: Evidence from Obsidian Hydration Studies

ALEXANDER K. ROGERS
100 E. Las Flores Ave.
Maturango Museum, Ridgecrest, CA 93555

ROBERT M. YOHE II
California State University, Bakersfield
Department of Sociology and Anthropology
9001 Stockdale Highway, Bakersfield, CA 93311

We report on a re-analysis of the obsidian from Rose Spring (CA-INY-372), Inyo County, California, based on obsidian hydration dating. The computed projectile point ages for Desert Series, Rose Spring Corner-Notched, Elko, and Humboldt Basal-Notched points fall within the expected range, which gives confidence in the analytic technique. The projectile points are younger than the debitage, even though both points and debitage experienced similar temperature histories, and the age difference is statistically significant at the 95% confidence level. Five of the Rose Spring Corner-Notched points show evidence of having been reworked from earlier points. The debitage age data also show a dependence on depth, but not as strongly as the radiocarbon data, probably due to vertical mixing. Both the mixing and the earlier age for the debitage suggest that tool stone on hand as debitage was salvaged and reutilized for tool manufacture, as a substitute for logistical traveling to gather lithic material from its source in the Coso volcanic field.

This paper briefly summarizes the results of a re-analysis of the obsidian hydration data from the Rose Spring site (CA-INY-372), in southern Inyo County, California (Fig. 1). Prior studies of obsidian quarrying in the Coso volcanic field have identified the utilization of Coso obsidian as early as the early Holocene (>8,500 radiocarbon years before present [rcybp], 9,492 cal B.P.), reaching a peak between 3,500 and 1,000 rcybp (3,778 and 911 cal B.P.; Gilreath and Hildebrandt 2011).

Figure 1. Location of CA-INY-372, Rose Spring.

Hildebrandt and McGuire (2002) analyzed over 100 single-component quarry loci, and found a significant peak in obsidian use between 2,300 and 1,275 rcybp (2,321–1,188 cal B.P.). Gilreath and Hildebrandt (2011:175) further show an almost complete cessation of quarrying and export of Coso obsidian post-650 rcybp (620 cal B.P.).

The Rose Spring site is not within the Coso quarry areas but is within 13 km. of it. The site consists of six loci (Fig. 2), with the obsidian samples for analysis being drawn from locus 1 (Fig. 3). Between two excavations (1951–1961 and 1987–1989) a total of 283 projectile points was recovered, 280 of which were obsidian (Yohe 1992). Among the assemblage were 12 Desert Side-Notched (DSN), 39 Cottonwood Triangular (CWT) or Leaf Shaped (CLS), 143 Rose Spring Corner-Notched (RSCN), 29 Elko (EL), 4 Gypsum Cave, 15 Humboldt Basal-Notched (HBN), 3 Pinto, one possible Silver Lake, and one possible fluted points (Yohe 1992).

Yohe (1998) conducted a detailed lithic analysis of the debitage assemblage from Rose Spring and concluded

Figure 2. Overview of Rose Spring (CA-INY-372). From Yohe 1992.

that the exploitation of Coso obsidian remained relatively stable through time, and that the lithic reduction strategy was minimally impacted by the introduction of archery. Allen (1986) reached a similar conclusion based on the assemblage from Coso Junction Ranch. Yohe's conclusion was based on a lack of change in the ratio of

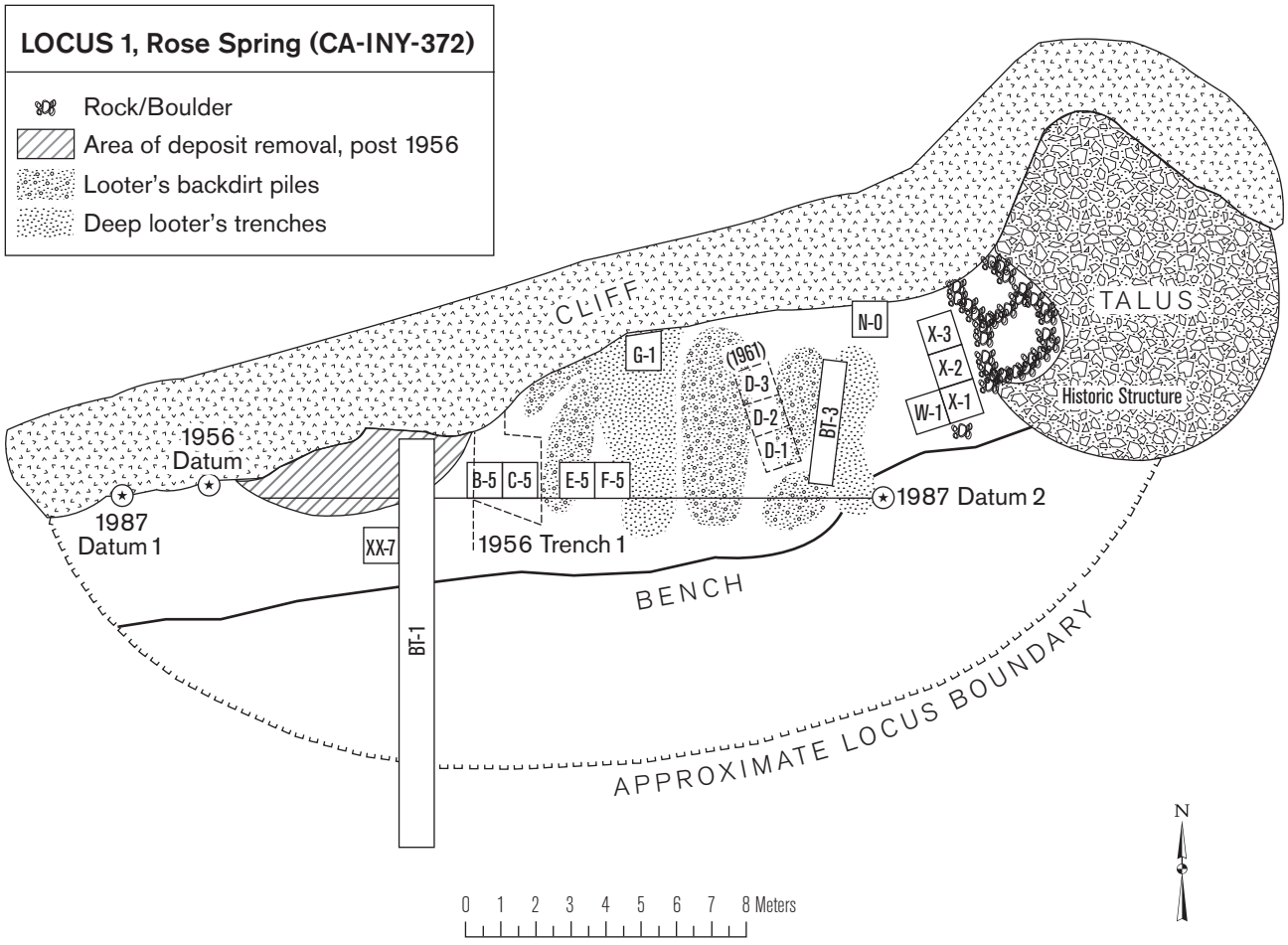

Figure 3. Locus 1 at Rose Spring, CA-INY-372. From Yohe 1992.

early- vs. late-stage thinning flakes present (Yohe 1998:43). However, he pointed out an alternate explanation in the conclusion to his paper—the possibility that significant mixing had occurred, "...incorporating debitage and bifaces from earlier periods of site use into the more recent cultural deposit" (Yohe 1998:49), and calling for further obsidian hydration dating (OHD) studies.

The present analysis responds to this need, based on data from Yohe (1992, 1998), and represents a significant refinement of the prior analyses reported in Rogers (2008a, 2009) and Garfinkel (2009). The data set analyzed here includes the debitage data reported by Yohe (1992:262–284, App. II) as well as the projectile point data of Yohe (1998:48, Table 10), augmented by the additional data on Rose Spring points from Garfinkel (2009:44, Table 1). All artifacts were geochemically sourced to the Coso volcanic field but not to a specific flow.

OBSIDIAN HYDRATION METHODS

Basis Of The Model

The basis of chronometric analysis using obsidian hydration is the equation

$$t = r_c^2/k \quad (1)$$

where t is age in calendar years, r_c is rim thickness in microns, and k is the hydration rate. Although other equations have been proposed (e.g., Basgall 1991; Pearson 1994), Equation 1 is the only form with both theoretical (Doremus 2002; Ebert et al. 1991) and laboratory (Doremus 1994; Stevenson et al. 1998, 2000) support.

The hydration rate is affected by five parameters: ground-water chemistry (Morgenstein et al. 1999); obsidian anhydrous chemistry (Friedman et al. 1966); obsidian intrinsic water content (Zhang et al. 1991; Zhang and Behrens 2000); humidity (Mazer et al. 1991); and

temperature (Hull 2001; Rogers 2007, 2012). Groundwater chemistry is only a factor in cases where potassium content is very high, as in some desert playas; otherwise it can be ignored. Obsidian anhydrous chemistry is controlled by sourcing the obsidian. The intrinsic water concentration can vary within an obsidian source (Stevenson et al. 1993), and can affect hydration rates significantly (Zhang et al. 1991; Zhang and Behrens 2000); there are no archaeologically appropriate techniques for measuring the intrinsic water at present, so its effects must be controlled statistically, by sample size. Humidity has a small effect which can generally be ignored.

Temperature is the major factor which needs to be controlled by computation in performing an obsidian hydration analysis. Archaeological temperatures vary both annually and diurnally, and the hydration rate is a strong function of temperature. The effective hydration temperature (EHT) is defined as a constant temperature which yields the same hydration results as the actual time-varying temperature over the same period of time. The mathematical derivation is given in Rogers (2007, 2012).

The exact solution for EHT requires integration of the temperature-dependent hydration rate over a time span in which the temperature varies diurnally and annually about an annual mean temperature (Rogers 2007, 2012). The computer code used in this analysis computes the integral as a finite sum.[1] The temperature is modeled as the sum of a mean temperature and two sinusoids, one with a 24-hour period and the other with a 12-month period. The time increment is one hour, and the period of integration is one year. The amplitudes of the mean and the two sinusoids are described below.

Temperature Parameters

Most archaeological sites are not located near meteorological stations, but temperature parameters for such sites can be estimated by regional temperature scaling (Rogers 2008b). It is important to use long-term data in these computations, and 30 years is the standard for determining climatological norms (Cole 1970). Such data can be down-loaded from the web site of the Western Regional Climate Center. The scaling principle assumes that desert temperature parameters are a strong function of altitude above mean sea level, and the best estimates of temperature are determined by scaling from 30-year data from a large number of meteorological stations.

Using this technique, in the northern Mojave Desert the annual average temperature can be predicted by the equation

$$T_a = 22.25 - 1.8h, \quad 0.94 \le h \le 11.8, \tag{2}$$

where h is altitude in thousands of feet. The accuracy of this model is 0.98ºC, 1-sigma.

The annual temperature variation can be predicted by

$$V_{a0} = 23.14 - 0.5h, \tag{3}$$

with h defined as above. The accuracy of the prediction is 0.27ºC, 1-sigma.

The best fit between V_d and altitude is relatively poor, and in the absence of other data about a site, the optimal estimate is

$$V_{d0} = 15.8ºC \tag{4}$$

for locations in the western Great Basin and deserts, irrespective of altitude. The accuracy of this estimate is 1.67ºC, 1-sigma. The overall accuracy of the EHT calculation is ~1°C, 1-sigma.

The elevation of the Rose Spring site, used in computing temperature parameters, is 3,584 ft. Equations 2–4 then yield the following data for this site: $T_a = 15.8°C$, $V_{a0} = 21.3°C$, and $V_{d0} = 15.8°C$.

These equations are for air temperatures. Obsidian on the surface is exposed to surface temperatures, which can be significantly higher than air temperatures in areas devoid of vegetation (Johnson et al. 2002; Rogers 2008c). However, a prior detailed analysis based on data from Rose Spring has shown that meteorological air temperature gives a good estimate of surface ground temperature in situations in which even intermittent shade is present (Rogers 2008a).

For buried artifacts, V_a and V_d represent the temperature variations at the artifact burial depth, which are related to surface conditions by

$$V_a = V_{a0}\exp(-0.44z) \tag{5a}$$

and

$$V_d = V_{d0}\exp(-8.5z) \tag{5b}$$

where V_{a0} and V_{d0} represent nominal surface conditions and z is burial depth in meters (Carslaw and Jaeger 1959:81). Depth correction for EHT is desirable, even in the presence of site turbation, because the depth correction, on the average, gives a better age estimate.

The computer code used here includes a first-order model of site formation processes by modeling the effects of the length of time an artifact was buried, as well as its depth. The user can input a value for the fraction of the time the artifact life was buried, based on archaeological evidence. The algorithm computes an average value of the diffusion coefficient over time and uses this value to compute age.

Temperature Correction of Hydration Data

Once the EHT has been computed, the measured rim thickness is multiplied by a rim correction factor (RCF) to make it comparable to those from a reference site:

$$RCF = \exp[(E/EHT_r) - (E/EHT)] \quad (6)$$

where EHT_r is the effective hydration temperature for the hydration rate (20°C here) and E is the activation energy of the obsidian (~10,000°K for Coso, per Friedman and Long 1976). The EHT-corrected rim value r_c is then

$$r_c = RCF \times r \quad (7)$$

The resulting values of r_c are then used in Equation 1 to compute age.

Since climate has not been stable over periods of archaeological interest, the effects of resulting temperature changes must be included in some cases. West et al. (2007:15, Fig 2.2 C, D) have published a reconstruction of variations in the regional-scale mean temperature since the late Pleistocene, based on multi-proxy data. Rogers (2010a) has developed a method for computing correction factors to adjust ages based on current conditions and account for paleotemperature variations. The effect is relatively small, <±7%, for ages back to 18,000 years. The computer code used in this analysis includes this paleotemperature correction.

Sources of Error

There are five primary sources of error (or uncertainty) in the parameters used for age computation: obsidian rim measurement; errors in the hydration rate ascribed to a source; intra-source rate variability due to uncontrolled intrinsic water in the obsidian (Ambrose and Stevenson 2004; Rogers 2008d; Stevenson et al. 1993, 2000; Zhang et al. 1991; Zhang and Behrens 2000); errors in reconstructing the temperature history; and association errors caused by site formation processes (Schiffer 1987). The effects of these errors have been examined in detail, with the analysis documented by Rogers (2010b).

Obsidian sample sizes are generally relatively small due to cost constraints, typically <10, while the uncertainty sources produce at least five degrees of freedom in the errors. For this reason, sample standard deviation is generally not a good estimate of age accuracy; a better strategy for estimating age accuracy is to use *a priori* information about the individual error sources, and infer the accuracy of the age estimate. The coefficient of variation of the age estimate, CVt, can be shown to be (Rogers 2010b)

$$CV_t^2 = 4[(\sigma_r/r)^2 + (0.06\sigma_{EHT})^2 + (CV_{ks}/2)^2 + CV_{ke}^2] \quad (8)$$

where the variables are defined as follows: σr is the standard deviation of the hydration rim measurement, and is ~0.1μ; r is the mean EHT-corrected hydration rim; σ_{EHT} is the uncertainty in EHT post-correction, and is ~1.0°C; CV_{ke} is the coefficient of variation of the hydration rate ascribed to the obsidian source, and is typically ~0.05; and CV_{ks} is the coefficient of variation of the intra-source rate variations, with a numerical value discussed below.

Once CV_t is computed from Equation 8, the standard deviation of the uncertainty in the age estimate is

$$\sigma_t = CV_t \times t \quad (9)$$

This is the accuracy figure quoted in the computer program output. The sample standard deviation is also provided for comparison.

ANALYSIS–PROJECTILE POINTS

The projectile point data set used for analysis is presented in Yohe (1998:48, Table 10) and Garfinkel (2009:44: Table 1), and is summarized in Table 1 (left five columns). The catalog numbers (Cat. Nos.) beginning with 131- are from Yohe, and the numbers beginning APG- are from Garfinkel.

In all, 44 points were cut for obsidian hydration analysis (Table 1). Six of the RSCN and one of the CLS points were cut a second time, to sample what appeared to be older surfaces on reworked points and to shed light on the rework trajectory hypothesis of Flenniken and Wilke (1989).

Three major analytic assumptions were made. First, although the artifacts were not sourced to a specific flow,

Table 1

PROJECTILE POINT HYDRATION DATA AND AGE RESULTS IN CAL B.P., ROSE SPRING (INY-372)

Cat. No.	Type	Cut No.	Test Unit	Depth, m.	R_{meas}, μ	R_{20}, μ	Mean Age cal B.P.	Sd_{mod}, yrs.
131-G1-121	DSN	1	G-1	0.00	2.3	2.26	287	77
131-B5-160-1	CLS	1	B-5	0.00	5.0	4.91	1,335	343
131-B5-160-2	CLS	2	B-5	0.00	7.6	7.47	3,148	803
131-F5-21	CWT	1	F-5	0.45	3.6	3.78	806	209
131-W1-98a	HBN	1	W-1	0.65	6.0	6.35	2,256	577
131-W1-98b	HBN	1	W-1	0.65	6.0	6.35	2,256	577
131-F5-36a	HBN	1	F-5	0.00	6.6	6.48	2,350	601
131-F5-36a	HBN	1	F-5	0.00	6.7	6.58	2,425	620
131-E5-100a	EL	1	E-5	1.65	7.6	8.24	3,850	982
131-E5-100b	EL	1	E-5	1.65	7.7	8.35	3,950	1,008
131-E5-59	EL	1	E-5	1.55	7.9	8.55	4,133	1,054
131-NO-19a-1	RSCN	1	N-O	0.05	5.1	5.15	1,476	379
131-NO-19a-2	RSCN	2	N-O	0.05	7.2	7.28	2,982	761
131-NO-19b-1	RSCN	1	N-O	0.05	5.2	5.26	1,537	395
131-NO-19b-2	RSCN	2	N-O	0.05	7.0	7.07	2,815	719
131-W1-65	RSCN	1	W-1	0.45	3.7	3.89	849	220
131-NO-80-1	RSCN	1	N-O	0.55	5.8	6.12	2,091	535
131-NO-80-2	RSCN	2	N-O	0.55	18.3	19.31	20,555*	5,221
131-X2-74	RSCN	1	X-2	0.35	3.4	3.56	717	187
131-XX7-72	RSCN	1	XX-7	0.65	5.7	6.04	2,034	521
APG-1	RSCN	1	unk	0.05	4.7	4.75	1,245	320
APG-2	RSCN	1	unk	0.05	4.6	4.65	1,193	307
APG-3-1	RSCN	1	unk	0.05	5.1	5.15	1,476	379
APG-3-2	RSCN	2	unk	0.05	7.2	7.28	2,982	761
APG-4-1	RSCN	1	unk	0.05	5.2	5.26	1,537	395
APG-4-2	RSCN	2	unk	0.05	7.0	7.07	2,815	719
APG-5	RSCN	1	unk	0.15	4.4	4.54	1,139	294
APG-6	RSCN	1	unk	0.15	4.5	4.65	1,191	307
APG-7	RSCN	1	unk	0.15	4.0	4.13	952	246
APG-8	RSCN	1	unk	0.25	3.0	3.12	557	146
APG-9	RSCN	1	unk	0.25	3.4	3.54	710	185
APG-10	RSCN	1	unk	0.25	4.9	5.10	1,443	371
APG-11	RSCN	1	unk	0.35	3.1	3.24	601	157
APG-12-1	RSCN	1	unk	0.35	4.1	4.29	1,021	264
APG-12-2	RSCN	2	unk	0.35	5.0	5.23	1,523	391
APG-13	RSCN	1	unk	0.35	3.4	3.56	717	187
APG-14	RSCN	1	unk	0.45	4.7	4.94	1,350	347
APG-15-1	RSCN	1	unk	0.45	4.5	4.73	1,234	318
APG-15-2	RSCN	2	unk	0.45	9.7	10.19	5,580	1,421
APG-16	RSCN	1	unk	0.45	2.7	2.84	458	121
APG-17	RSCN	1	unk	0.45	4.5	4.73	1,234	318
APG-18-1	RSCN	1	unk	0.45	4.3	4.52	1,127	291
APG-18-2	RSCN	2	unk	0.45	6.0	6.31	2,221	568
APG-19	RSCN	1	unk	0.45	4.8	5.04	1,411	363
APG-20	RSCN	1	unk	0.45	5.0	5.25	1537	395
APG-21	RSCN	1	unk	0.45	3.7	3.89	849	220
APG-22	RSCN	1	unk	0.55	3.7	3.90	855	222
APG-23	RSCN	1	unk	0.55	4.3	4.54	1,137	293
APG-24	RSCN	1	unk	0.55	5.8	6.12	2,091	535
APG-25	RSCN	1	unk	0.65	5.0	5.30	1,562	401
APG-26	RSCN	1	unk	0.65	5.7	6.04	2,034	521
APG-27	RSCN	1	unk	0.85	4.4	4.69	1,214	313
APG-28	RSCN	1	unk	1.05	5.0	5.36	1,601	411

*Excluded from the analysis; see discussion in text below. unk=unknown

Table 2

PROJECTILE POINTS FROM THE ROSE SPRING SITE (INY-372), HYDRATION RIM STATISTICS (MICRONS)

	RSCN, First Cut, Mod Data Set		RSCN, Second Cut, Mod Data Set		HBN		ELKO	
	R_{meas}	R_{20}	R_{meas}	R_{20}	R_{meas}	R_{20}	R_{meas}	R_{20}
Mean	4.51	4.71	7.62	7.78	6.33	6.44	7.73	8.38
Sample SD	0.85	0.89	1.17	1.35	0.38	0.11	0.15	0.16
CV	0.19	0.19	0.15	0.17	0.06	0.02	0.02	0.02
Max	5.80	6.31	9.70	10.19	6.60	6.58	7.90	8.55
Min	2.70	2.84	7.00	7.07	6.00	6.35	7.60	8.24
N	36	36	5	5	4	4	3	3

other obsidian assemblages from the Rose Valley area are composed primarily of glass from the West Sugarloaf flow; thus, the hydration rate used in this analysis is that for West Sugarloaf (18.14 μ^2/1000 yrs. at 20°C, with a CV_{ks} of 0.20, from Rogers 2013). Second, the assumption was made that each artifact was buried at its recovery depth for one-half its life, and on the surface the other half, since turbation had clearly occurred (Yohe 1992). The EHT was then computed on this basis. Third, the laboratory measurement error standard deviation was assumed to be 0.1μ, based upon standard laboratory practice.

The resulting corrected rim data are presented in Table 1 (right three columns). In the table, R_{meas} refers to the hydration rim as measured and reported by a laboratory; R_{20} refers to the hydration rim corrected to 20°C, including depth and site formation corrections; mean age is in calibrated years before 2,000 (=cal B.P.); "Sd_{mod}" is the age error standard deviation from Equations 8 and 9 above. The table entries where the test unit is noted as "unk" occur because the test unit data were not included in Garfinkel (2009).

Several points may be adduced from these data. First, the second cut on RSCN point Cat. No. 131-N0-80-2 exhibits a hydration rim which is considerably too large (20,555 ± 5,221 cal B.P.). It is probably a geologic surface, and although it cannot be excluded by Chauvenet's criterion, it is excluded judgmentally from further analysis. In addition, the DSN, CWT, and CLS points are not considered, due to small sample sizes.

Analysis of the EHT-corrected hydration rim data (R_{20}) for the RSCN points shows that there is a small amount of overlap between the data from cut #1 and cut #2. The second cuts on Cat. Nos. APG-12-2 and APG-18-2 fall within the range of values for the first cuts, and are separated from the remainder of the second cuts by a gap. Thus, these two have been judgmentally included in the "first cut, modified" data set below, yielding an N=36. If these points were reworked from an earlier point, cut #2 may have sampled a fresh surface.

Further, the single cut on Cat. No. APG-15-2 falls far outside the range of first cuts, and possibly represents an un-reworked surface on a reworked point; it is grouped with the second cuts for analysis purposes, yielding N=5.

Table 2 summarizes the hydration rim data for the RSCN, HBN, and Elko points. Comparison of the R_{meas} and R_{20} statistics shows that the inclusion of burial depth causes significant changes in the corrected rim values. Sample size is designated by N.

For the RSCN and Elko points, the EHT correction has caused a shift in the mean value of hydration rim, although the coefficient of variation (CV) remains essentially the same. The case of HBN points is different: the mean changes very little, but the EHT correction reduces the CV by a factor of 3. *These observations show that it is inaccurate to base assessments on raw rim readings and on an assumed hydration rate; valid conclusions require the application of EHT corrections, including burial effects, to the data.*

Table 2 also shows that the first and second cuts on the RSCN points give greatly different figures, and the difference between the readings is statistically significant at the 95% confidence level (t=5.67, threshold=1.96). Thus, the modified first and second cut reading data sets should not be combined in analyses, but assessed separately. (Excluding point Cat. No. APG-15-2 from the second cut data set yields t=2.96, and does not alter this conclusion). The second cuts clearly represent an earlier episode of manufacture (Flenniken and Wilke 1989).

Table 3

OHD AGES IN YEARS CAL BP FOR POINTS FROM ROSE SPRING (INY-372)

	RSCN, First Cut, Mod Data Set	RSCN, Second Cut, Mod Data Set	HBN	ELK
Mean	1,276	3,435	2,322	3,978
SD_m	458	1202	82	144
SD_{agg}	570	1825	691	1,252
PE_{agg}	95	912	345	723
N	36	5	4	3

Turning to the computed ages, Table 3 summarizes statistics by point type. Ages are in cal B.P. "SD_m" is the standard deviation of the mean ages from Table 1. "SD_{agg}" is the standard deviation computed by including both the varying mean values and the standard deviations.[2] "PE_{agg}" is the probable error of the estimate of the mean, computed from SD_{agg} and sample size, and N is the number of measurements.

The ages seem to fall where expected, with the exception of the second cuts on the RSCN points (Justice 2002). It is likely that these represent cuts on an old surface, as would occur with an earlier point or flake being reworked into a RSCN (Flenniken and Wilke 1989). On the other hand, the second cuts on Cat. Nos. APG-13 and APG-32 are consistent with the first cuts, suggesting that the surfaces were contemporaneous.

The average age of all projectile points (including all cuts on all points except the second cut on Cat. No. 131-N0-80-2) is 1,729 ± 1,166 cal B.P. (N = 52, PE = 161 yrs.), with the standard deviation being the SD_{agg}, as defined above. The standard deviation of the means is 1,055 yrs.

ANALYSIS–DEBITAGE

The data set used for the analysis is presented in Yohe (1992:262–284, App. II) and is summarized in Table 4 below (left five columns). Flakes for hydration analysis were selected randomly by level (three each); the flakes represent specimens which are large enough for cutting and reading, and hence very small flakes were not selected. The debitage samples were taken from unit X-1 as it showed minimal damage from looters; however, it was found that X-1 only extended 160 cm. in depth, so a deeper sample was taken from unit XX-7 (Yohe 1992). The specimens from X-1 were read by Biosystems Laboratory, Inc., and those from XX-7 by the Obsidian Hydration Laboratory at the University of California, Los Angeles (Yohe 1992).

Individual debitage flakes are not temporally diagnostic in themselves, so the hydration rim data were aggregated by level for analysis. Data coverage from the two units overlaps at the 160, 170, 180, 190, and 200 cm. levels. A t-test shows that the data for 180, 190, and 200 cm. levels are statistically indistinguishable at the 95% confidence level, so they were aggregated by level between the two units to increase sample size. The same test showed that the data for the 160 and 170 cm. levels are statistically distinguishable at the 95% confidence level, so the samples were kept separate.

In seven cases dual readings were made on a flake; in each case a t-test showed the second reading to be statistically indistinguishable from the other readings at the same level at the 95% confidence level, so the second readings were combined with the first readings. The total number of hydration readings is 99; when aggregated by level as shown in Table 4 the number of analysis samples is 28, with sample sizes varying from N = 2 to N = 8.

Analytic assumptions, methods, and notations are the same as for projectile points. In this case, since the sample sizes are greater than unity, the sample standard deviation is shown; probable error is computed from the model standard deviation (Equations 8 and 9). The resulting corrected rims and ages (cal B.P.) are presented in Table 4 (right five columns).

Overall, the debitage exhibits an age of 3,159 ± 1,312 cal B.P., with the standard deviation being SD_{agg} and PE_{agg} = 132 yrs; the standard deviation of the debitage mean ages is 832 yrs. The distribution of ages is as expected for Coso obsidian samples, based on typical obsidian chemistry and EHT uncertainties (Rogers 2008d; Stevenson et al. 1993). The debitage ages are shown in Figure 4 in order of increasing age, showing that there is only one age less than 2,200 cal B.P.

ANALYSIS–COMPARISON

A comparison of the age distributions for debitage and projectile points reveals significant differences; the data are summarized in Table 5.

A t-test shows that the means are statistically distinguishable at the 95% confidence level (t = 5.04). The

Table 4

ROSE SPRING DEBITAGE DATA

Seq. No.	Test Unit	Depth, m.	N	R_{meas}, μ	Sample SD μ	R_{20}, μ	Age cal B.P.	S_{dmod}, yrs.	Sample SD, yrs.	PE, yrs.
1	X-1	0.05	3	6.67	2.08	6.74	2,544	650	1,590	375
2	X-1	0.15	3	7.93	1.87	8.19	3,802	970	1,794	560
3	X-1	0.25	3	6.57	1.48	6.83	2,620	670	1,184	387
4	X-1	0.35	3	6.20	0.90	6.49	2,352	602	683	347
5	X-1	0.45	4	3.35	1.35	3.52	704	184	566	92
6	X-1	0.55	3	7.07	1.77	7.46	3,140	802	1,570	463
7	X-1	0.65	3	6.97	0.06	7.38	3,070	784	51	453
8	X-1	0.75	3	5.93	1.63	6.31	2,221	568	1,217	328
9	X-1	0.85	3	6.00	0.52	6.40	2,287	585	396	338
10	X-1	0.95	3	6.27	1.80	6.70	2,515	643	1,445	371
11	X-1	1.05	3	7.47	0.55	8.00	3,630	926	536	535
12	X-1	1.15	3	7.00	0.10	7.52	3,194	816	91	471
13	X-1	1.25	3	7.17	1.40	7.72	3,370	860	1,318	497
14	X-1	1.35	3	7.27	0.21	7.84	3,481	889	199	513
15	X-1	1.45	4	6.75	1.11	7.30	2,998	766	988	383
16	X-1	1.55	4	7.43	1.29	8.04	3,664	935	1,270	467
17	X-1	1.65	3	7.23	0.71	7.84	3,485	890	684	514
18	XX-7	1.65	3	6.43	0.06	6.98	2,734	699	49	404
19	X-1	1.75	4	8.78	1.40	9.53	4,965	1,265	1,585	633
20	XX-7	1.75	3	6.47	0.81	7.02	2,770	708	693	409
21	Comb.	1.85	6	7.27	0.95	7.90	3,536	903	923	368
22	Comb.	1.95	8	6.84	1.30	7.44	3,128	799	1,187	283
23	Comb.	2.05	5	6.74	0.98	7.34	3,043	777	886	348
24	XX-7	2.15	3	8.43	0.49	9.20	4,673	1,191	547	688
25	XX-7	2.25	3	8.13	0.29	8.88	4,416	1,126	314	650
26	XX-7	2.35	4	6.23	1.48	6.80	2,596	664	1,234	332
27	XX-7	2.45	2	7.15	0.21	7.82	3,463	884	205	625
28	XX-7	2.55	4	7.63	0.67	8.34	3,945	1,006	693	503

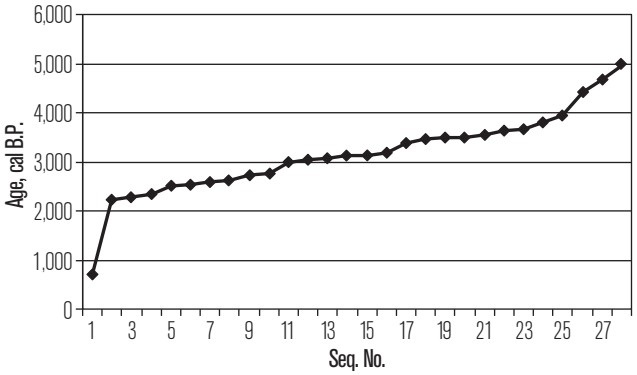

Figure 4. Debitage age distribution based on OHD. Note the abrupt decline post-2,200 cal B.P. and that there is only one date after this point.

Table 5

OHD AGES FOR DEBITAGE AND PROJECTILE POINTS, CAL B.P.

	Debitage Sample Ages, Yrs.	Projectile Point Ages, Yrs.
Mean	3,216	1,729
SD_m	783	1,055
SD_{agg}	1,306	1,166
N	28	52

t-test is based on the conservative assumption that SD_{agg} is the appropriate measure of dispersion; if SD_m is used the value of t is larger.

The difference can be viewed graphically as a histogram, with the ages grouped by archaeological period (Fig. 5). Table 6 presents the ages as histogram data, grouped by archaeological period. Figure 5 clearly shows that the central tendency of the age of the projectile points is younger than that of the debitage.

The difference can also be shown by means of a Kolmogorov-Smirnov analysis, by computing a cumulative distribution from the fraction data of Table 6 (Fig. 6). The maximum difference between the curves is 0.62; the threshold for distinguishability at the 95% confidence level is 0.32. Thus, the distribution of debitage ages is older than the projectile point ages, with a confidence in excess of 95%. The cultural implications of this difference are discussed below.

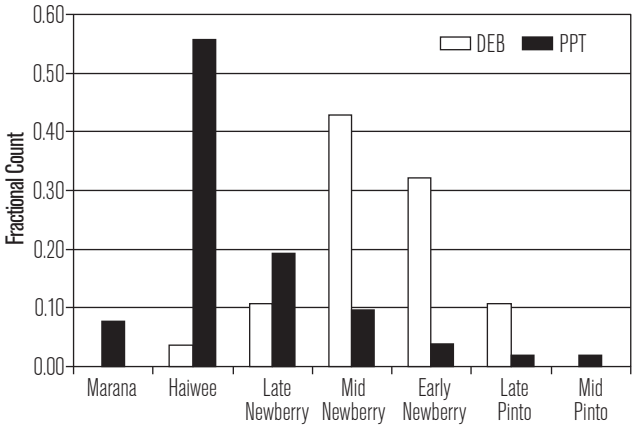

Figure 5. Comparison histogram of debitage ages and projectile point ages from Rose Spring. Ages based on OHD.

Table 6

ROSE SPRING OHD AGES

Period	Start Date, cal B.P.	Debitage Sample Count	Debitage Fraction	Projectile Point Count	Projectile Point Fraction
Marana	700	0	0.00	4	0.08
Haiwee	1,600	1	0.04	29	0.56
Late Newberry	2,500	3	0.11	10	0.19
Mid Newberry	3,200	10	0.36	5	0.10
Early Newberry	4,000	11	0.39	2	0.04
Late Pinto	5,000	2	0.07	1	0.02
Mid Pinto	6,000	1	0.04	1	0.02

DEPTH DEPENDENCE

The dependence of specimen age on burial depth differs significantly between the radiocarbon samples and obsidian dates (Fig. 7). The radiocarbon dates were obtained from ten hearth features and seven loose charcoal specimens. Loose charcoal is more susceptible to bioturbation than are hearths, so this discussion is based on hearth data only. The linear least-squares best fit to the hearth data set has a slope of 1,967 radiocarbon years/m. depth and a y-intercept of –982 rcybp; $R^2 = 0.95$, showing the fit is quite good. The negative y-intercept

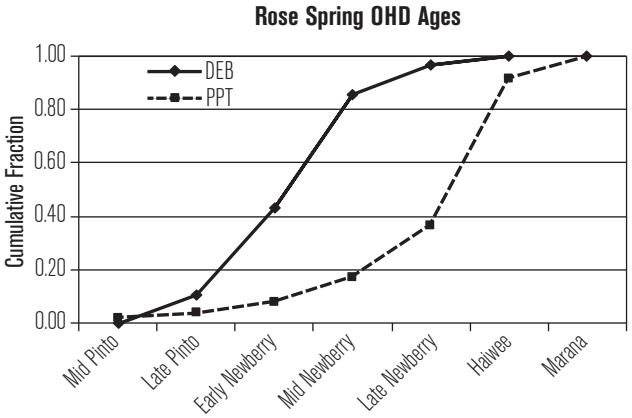

Figure 6. OHD ages from Rose Spring, plotted as cumulative fractions. The curves are distinguishable at the 95% confidence level.

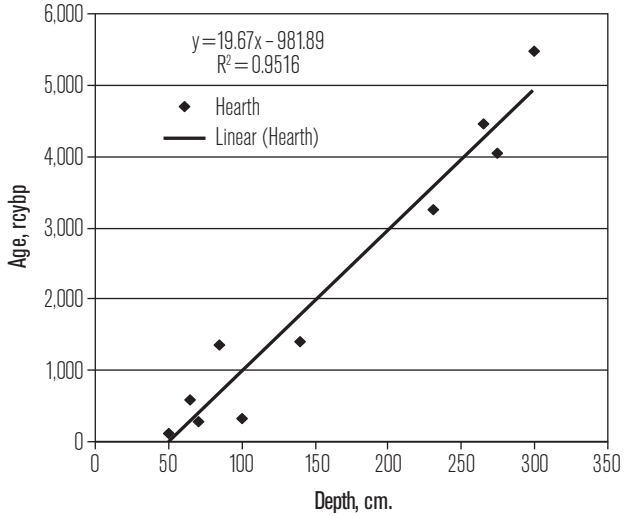

Figure 7. Radiocarbon ages vs. depth for Locus 1, Rose Spring (INY-372), showing data from hearth sources only. Radiocarbon ages lack $\delta^{13}C$ correction. Data from Yohe (1992).

implies that the best fit line crosses the x-axis at a positive value, which corresponds to the "radiocarbon present." In this case, the radiocarbon present is approximately 50 cm. below the present ground surface. This suggests either aggradation of the surface or downward movement of the radiocarbon specimens has occurred; since the hearths which yielded the samples are intact, aggradation is more likely, and in fact can be observed at the site today as deep sheet-wash.

By contrast, the variation of hydration ages with depth is less distinct (Fig. 8). The slope is much less steep, with a slope of only 574 radiocarbon years/m. depth, and a y-intercept of 2,393 rcybp; the value of R^2 is only 0.26. The positive y-intercept equates to a "present" at a negative depth, which implies either surface degradation or upward movement of the specimens. Since the radiocarbon data, and current observations at the site, both show that aggradation is occurring, vertical movement of the obsidian must have occurred. A general upward movement of older obsidian, such as would occur if obsidian were being salvaged, would have the effect of flattening the slope and creating an apparent negative "surface" level.

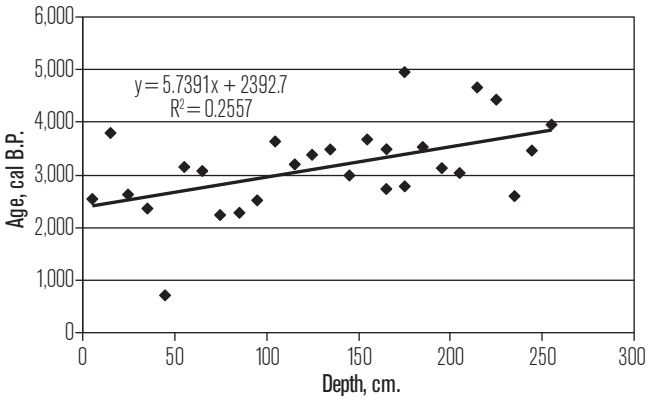

Figure 8. Depth dependence of OHD ages of debitage from Locus 1 at Rose Spring (INY-372).

DISCUSSION

The data presented here show that the ages for Rose Spring Corner-Notched (1,276 ± 570 cal B.P., N = 36), Elko (3,978 ± 1,252 cal B.P., N = 3), and Humboldt Basal-Notched (2,322 ± 691 cal B.P., N = 4) points fall where expected. In each case the standard deviations include the variations expected from the chemistry of the Coso source, in addition to the standard deviations of the means, and thus are conservative.

Furthermore, despite small sample sizes (N = 1), the age for a Desert Side-Notched point (287 ± 77 cal B.P.) is reasonable; the age for the Cottonwood Triangular point (806 ± 209 cal B.P.) is somewhat old, but possible in view of the uncertainties with regard to the obsidian and the possibility that the hydration cut sampled an older surface on a reworked point or flake.

The ages computed from five of the second cuts on the RSCN points are exceptions, as they are Newberry age or older. The second cut on Cat. No. 131-N0-80 is clearly on a geologic surface, and it has been excluded from the analyses here. In two other cases (Cat. Nos. APG-12-2 and APG-18-2), the ages fall within the range of the first cuts, and thus represent surfaces contemporaneous with the first cuts. In the other four cases (Cat. Nos. 131-N0-19b, 131-N0-19a, APG-3, APG-18), the second ages average 2,319 ± 1,090 cal B.P. (N = 4), which is mid-Newberry period. Addition of Cat. No. APG-15-2 raises the age to 3,435 ± 1,202 cal B.P. It is likely that the surface sampled by these cuts was an un-reworked surface, such as would occur on an RSCN reworked from an earlier point or a salvaged flake, supporting the rework model of Flenniken and Wilke (1989).

The debitage ages are generally older than the projectile point ages. This is evidenced by the age statistics (3,216 ± 1,306 cal B.P. for debitage vs. 1,729 ± 1,166 cal B.P. for all projectile points), a difference which is statistically significant by t-test at the 95% confidence level. In addition, the cumulative fraction plots clearly show the offset in age, which is statistically significant by the Kolmogorov-Smirnov test at the 95% confidence level.

The difference between the mean ages of Elko points and the debitage is not statistically significant (t = 1.00, threshold = 1.96), suggesting that the debitage and the Elko points were produced at the same time, probably from bifacial cores transported from the Coso quarries. The difference between the mean ages of debitage and Humboldt points is statistically significant (t = 2.11, threshold = 1.96); however, the debitage age overlaps and completely encompasses the hydration ages of the Humboldt points, suggesting again that some of these points could have been produced from bifacial cores from the quarries.

The situation is different for the arrow-size points. The obsidian hydration ages of Rose Spring Corner-Notched points and debitage are significantly different (t=7.34, threshold=1.96), and there is virtually no overlap in the data sets. It is thus highly unlikely that the points and debitage were produced in the same episode, and reinforces the view that the points were produced later from salvaged material.

The debitage age data show some degree of dependence on depth, but not as strongly as do the radiocarbon data. Furthermore, extrapolation of obsidian ages to a zero age results in a negative apparent "surface" depth; i.e., above the present ground surface. However, both radiocarbon and current observations of the site show the surface is aggrading. The obsidian dates would be explained if the older obsidian was being dug up and re-used even on the aggraded surface in later times. The behavior envisioned involves the site occupants digging or scraping the ground surface to obtain suitable tool stone for the manufacture of projectile points and other small tools, then leaving the debitage where it fell.

Such a reuse of tool stone should have also resulted in creating younger debitage. However, the scavenged obsidian was certainly smaller than a fresh bifacial core, and the tools being manufactured were probably mostly small, such as arrow-size points. The resulting debitage would be smaller in quantity than that from bifacial core reduction. It would also be smaller in size, and less likely to have been selected as a specimen for hydration measurement, which requires specimens large enough to cut and read.

CONCLUSIONS

The fact that the OHD analytical process employed here yields archaeologically reasonable ages for temporally-sensitive projectile points gives a degree of confidence that the analytical technique is valid. Furthermore, the debitage sample is from the same source as the projectile points, and has experienced essentially the same temperature history, which gives confidence in the debitage dates.

Since the debitage is clearly older than the projectile points, and some Haiwee-period points preserve Newberry-period surfaces, a reasonable inference is that obsidian debitage and curated or broken points from Newberry times were being recycled in Haiwee and Marana times, instead of bifacial cores being imported from the Coso quarries for tool manufacture. This inference is reinforced by the age-vs.-depth data, which indicate significant vertical mixing of the obsidian debitage, as would be caused by digging to recover debitage for tool manufacture.

A final consideration is provided by local geography. Even though the Rose Spring site is relatively near the obsidian sources at the Coso volcanic field, the round-trip distance is still approximately 25 km.; for hunter-gatherers traveling on foot, this distance would tend to discourage unnecessary trips, and encourage the scavenging and re-use of tool stone on hand. Any gathering of tool stone from Coso would require organized logistical foraging, and was probably not done often. From an optimal foraging standpoint, re-using tool stone on hand would greatly reduce energy expenditures.

It thus appears that Yohe's alternate explanation (Yohe 1998:49) is valid. The detailed obsidian hydration analysis shows the presence of significant vertical mixing of the obsidian debitage samples; it also shows that the mean debitage age is older than the mean projectile point age, and that there was a change in lithic production strategies at the time archery was introduced.

ACKNOWLEDGMENTS

We acknowledge with gratitude the work of the GIS wizards at Epsilon Systems—Daniel Veazey, Justin Pooley, and Vitaty Deakin—who created the maps for Figures 1–3. We further acknowledge with thanks the insightful comments of Matt Hall and another, anonymous, reviewer, which have significantly improved the quality of this paper. Any remaining faults, whether of omission or commission, are of course ours.

NOTES

[1]The computer code is written in MatLab®; users having access to MatLab can obtain a copy of the computer code by contacting the primary author.

[2]Mean and standard deviation for aggregated statistics:

Given a collection of N data sets, with statistics defined as follows:

m_i = mean for the ith data set
σ_i = standard deviation for the ith data set
n_i = sample size for the ith data set.
N = number of data sets, so i = 1, 2, 3, …, N

The overall mean M of the aggregated data set is the weighted average

$$M = (\Sigma\, n_i\, m_i) / \Sigma\, n \qquad \text{(A-1)}$$

where the summation is taken over i = 1 to N.

The variance S2 of the aggregated data set is

$$S^2 = [\Sigma n_i (m_i - M)^2 + \Sigma n_i \sigma_i^2] / \Sigma\, n_i \qquad \text{(A-2)}$$

where the summation is again taken over i = 1 to N. The aggregate standard deviation SD_{agg} is

$$SD_{agg} = \sqrt{(S^2)}\ . \qquad \text{(A-3)}$$

The computed value of S_{agg} gives the standard deviation of the aggregate of the data sets, and yields the same result as if the standard deviation were computed from the detailed data.

Finally, the probable error of the aggregate PE_{agg} is

$$PE_{agg} = S_{agg} / \sqrt{(N)} \qquad \text{(A-4)}$$

It is thus the probable error of the mean estimate, taking into account the standard deviations of the data sets, and not simply the standard deviation of the means. Equations A-1 through A-4 can be conveniently implemented in MS Excel.

For the case of the present OHD analysis, the mean and standard deviation of the projectile point ages ($n_i = 1$ in each case) is computed from the known properties of Coso obsidian, probable errors in EHT (assumed to be ~1°C), and lab measurement errors in measuring hydration rims (assumed to be ~0.1μ) (Rogers 2008c, 2010b).

REFERENCES

Ambrose, W. R., and C. M. Stevenson
2004 Obsidian Density, Connate Water, and Hydration Dating. *Mediterranean Archaeology and Archaeometry* 4(2):5–16.

Allen, Mark W.
1986 *The Effects of Bow and Arrow Technology on Lithic Production and Exchange Systems: A Test Case Using Debitage Analysis.* Master's thesis, University of California, Los Angeles.

Basgall, Mark E.
1991 Hydration Dating of Coso Obsidian: Problems and Prospects. Paper presented at the Annual Meeting of the Society for California Archaeology, Foster City.

Carslaw, H. S., and J. C. Jaeger
1959 *Conduction of Heat in Solids*, 2nd ed. Oxford: Clarendon Press.

Cole, F. W.
1970 *Introduction to Meteorology*. New York: Wiley.

Doremus, R. H.
1994 *Glass Science*, 2nd ed. New York: Wiley Interscience.
2002 *Diffusion of Reactive Molecules in Solids and Melts*. New York: Wiley Interscience.

Ebert, W. L., R. F. Hoburg, and J. K. Bates
1991 The Sorption of Water on Obsidian and a Nuclear Waste Glass. *Physics and Chemistry of Glasses* 34(4): 133–137.

Flenniken, J. J., and P. J. Wilke
1989 Typology, Technology, and Chronology of Great Basin Dart Points. *American Anthropologist* 91(1):149–158.

Friedman, I., and W. D. Long
1976 Hydration Rate of Obsidian. *Science* 191(1):347–352.

Friedman, Irving, Robert I. Smith, and William D. Long
1966 Hydration of Natural Glass and Formation of Perlite. *Geological Society of America Bulletin* 77:323–328.

Garfinkel, Alan P.
2009 Rose Spring Chronology and Numic Population Movements in Eastern California. *Pacific Coast Archaeological Society Quarterly* 43(1 & 2):42–49.

Gilreath, Amy G., and William R. Hildebrandt
1997 Prehistoric Use of the Coso Volcanic Field. *Contributions of the University of California Archaeological Research Facility* 56. Berkeley.
2011 Current Perspectives on the Production and Conveyance of Coso Obsidian. In *Perspectives on Trade and Exchange in California and the Great Basin*, Richard E. Hughes, ed., pp. 171–188. Salt Lake City: University of Utah Press.

Hildebrandt, William R., and Kelly R. McGuire
2002 The Ascendance of Hunting during the California Middle Archaic: An Evolutionary Perspective. *American Antiquity* 67:231–256.

Hull, Kathleen L.
2001 Reasserting the Utility of Obsidian Hydration Dating: A Temperature-Dependent Empirical Approach to Practical Temporal Resolution with Archaeological Obsidians. *Journal of Archaeological Science* 28:1025–1040.

Johnson, Michael J., Charles J. Mayers, and Brian J. Andraski
2002 *Selected Micrometeorological and Soil-Moisture Data at Amargosa Desert Research Site in Nye County near Beatty, Nevada, 1998–2000*. [*U.S. Geological Survey Open-File Reports* 02-348.] Carson City, Nevada. (With CD containing meteorological data records).

Justice, Noel D.
2002 *Stone Age Spear and Arrow Points of California and the Great Basin*. Bloomington: Indiana University Press.

Mazer, J. J., C. M. Stevenson, W. L. Ebert, and J. K. Bates
1991 The Experimental Hydration of Obsidian as a Function of Relative Humidity and Temperature. *American Antiquity* 56(3):504–513.

Morgenstein, M. E., C. L. Wickett, and A. Barkett
1999 Considerations of Hydration-Rind Dating of Glass Artefacts: Alteration Morphologies and Experimental Evidence of Hydrogeochemical Soil-zone Pore Water Control. *Journal of Archaeological Science*. 26(1999):1193–1210.

Pearson, James L.
1995 *Prehistoric Occupation at Little Lake, Inyo County, California: A Definitive Chronology*. Master's thesis, California State University, Los Angeles.

Rogers, Alexander K.
2007 Effective Hydration Temperature of Obsidian: A Diffusion-Theory Analysis of Time-Dependent Hydration Rates. *Journal of Archaeological Science* 34:656–665.
2008a An Evaluation of Obsidian Hydration Dating as a Chronometric Technique, Based on Data from Rose Spring (CA-INY-372), Eastern California. *Bulletins of the International Association for Obsidian Studies* 40:12–32.
2008b Regional Scaling for Obsidian Hydration Temperature Correction. *Bulletins of the International Association for Obsidian Studies* 39:15–23.
2008c Field Data Validation of an Algorithm for Computing Effective Hydration Temperature of Obsidian. *Journal of Archaeological Science* 35:441–447.
2008d Obsidian Hydration Dating: Accuracy and Resolution Limitations Imposed by Intrinsic Water Variability. *Journal of Archaeological Science* 35:2009–2016.
2009 An Estimate of Coso Obsidian Hydration Rate, Based on Obsidian-Radiocarbon Pairings and the "Weighted Total Least Squares" Method. *Bulletins of the International Association for Obsidian Studies* 41:9–20.
2010a How Did Paleotemperature Change Affect Obsidian Hydration Rates? *Bulletins of the International Association for Obsidian Studies* 42:13–20.
2010b Accuracy of Obsidian Hydration Dating based on Radiocarbon Association and Optical Microscopy. *Journal of Archaeological Science* 37:3239–3246.
2012 Temperature Correction for Obsidian Hydration Dating, In *Obsidian and Ancient Manufactured Glasses*, Ioannis Liritzis and Christopher Stevenson, eds., pp. 46–56. Albuquerque: University of New Mexico Press.
2013 Flow-Specific Hydration Rates for Coso Obsidian. *Proceedings of the Society for California Archaeology* 27 (in press).

Rogers, Alexander K., and Robert M. Yohe II
2011 An Improved Equation for Coso Obsidian Hydration Dating, based on Obsidian-Radiocarbon Association. *Proceedings of the Society for California Archaeology* 25. (Available on-line.)

Schiffer, Michael E.
1987 *Site Formation Processes of the Archaeological Record*. Salt Lake City: University of Utah Press.

Stevenson, Christopher M., E. Knauss, J. J. Mazer, and J. K. Bates
1993 The Homogeneity of Water Content in Obsidian from the Coso Volcanic Field: Implications for Obsidian Hydration Dating. *Geoarchaeology* 8(5):371–384.

Stevenson, Christopher M., J. J. Mazer, and B. E. Scheetz
1998 Laboratory Obsidian Hydration Rates: Theory, Method, and Application. In *Archaeological Obsidian Studies: Method and Theory. Advances in Archaeological and Museum Science, Vol. 3*, M. S. Shackley, ed., pp.181–204. New York: Plenum Press.

Stevenson, Christopher M., Mike Gottesman, and Michael Macko
2000 Redefining the Working Assumptions for Obsidian Hydration Dating. *Journal of California and Great Basin Anthropology* 22(2):223–236.

West, G. J., W. Woolfenden, J. A. Wanket, and R. S. Anderson
2007 Late Pleistocene and Holocene Environments. In *California Prehistory: Colonization, Culture, and Complexity*, T. L. Jones and K. A. Klar, eds., pp. 11–34. Walnut Creek: Altamira Press.

Yohe, Robert M., II
1992 *A Reevaluation of Western Great Basin Cultural Chronology and Evidence for the Timing of the Introduction of the Bow and Arrow to Eastern California Based on New Excavations at the Rose Spring Site (CA-INY-372)*. Ph.D. dissertation, University of California, Riverside.
1998 The Introduction of the Bow and Arrow and Lithic Resource Use at Rose Spring (CA-INY-372). *Journal of California and Great Basin Anthropology* 20(1):26–52.

Zhang, Y., E. M. Stolper, and G. J. Wasserburg
1991 Diffusion of Water in Rhyolytic Glasses. *Geochimica et Cosmochimica Acta* 55:441–456.

Zhang, Y., and H. Behrens
2000 H_2O Diffusion in Rhyolitic Melts and Glasses. *Chemical Geology* 169:243–262.